16. M. Y. Zhu, J. M. Zhang, A. H. Yang, *Palaeogeogr. Palaeoclimatol. Palaeoecol.* **254**, 7 (2007).
17. E. Vernhet, C. Heubeck, M. Y. Zhu, J. M. Zhang, *Precambrian Res.* **148**, 32 (2006).
18. D. J. Des Marais, H. Strauss, R. E. Summons, J. M. Hayes, *Nature* **359**, 605 (1992).
19. L. Yin *et al.*, *Nature* **446**, 661 (2007).
20. S. Xiao, Y. Zhang, A. H. Knoll, *Nature* **391**, 553 (1998).
21. G. D. Love *et al.*, *Nature* **457**, 718 (2009).
22. P. A. Cohen, A. H. Knoll, R. B. Kodner, *Proc. Natl. Acad. Sci. U.S.A.* **106**, 6519 (2009), and references therein.
23. D. E. Canfield, *Am. J. Sci.* **304**, 839 (2004).
24. J. L. Kirschvink, in *The Proterozoic Biosphere: A Multidisciplinary Study*, J. W. Schopf, C. Klein, D. Des Maris, Eds. (Cambridge Univ. Press, Cambridge, 1992), pp. 51–52.
25. M. T. Hurtgen, M. A. Arthur, N. S. Suits, A. J. Kaufman, *Earth Planet. Sci. Lett.* **203**, 413 (2002).
26. P. Gorjan, J. J. Veevers, M. R. Walter, *Precambrian Res.* **100**, 151 (2000).
27. L. R. Kump, W. E. Seyfried Jr., *Earth Planet. Sci. Lett.* **235**, 654 (2005).
28. K. S. Habicht, M. Gade, B. Thamdrup, P. Berg, D. E. Canfield, *Science* **298**, 2372 (2002).
29. D. H. Rothman, J. M. Hayes, R. E. Summons, *Proc. Natl. Acad. Sci. U.S.A.* **100**, 8124 (2003).
30. R. A. Berner, R. Raiswell, *Geology* **12**, 365 (1984).
31. We are extremely grateful to R. Raiswell, S. Bates, W. Gilhooly, B. Gill, J. Owens, A. Khong, P. Marenco, N. Planavsky, C. Reinhard, M. Rohrssen, C. Scott, S. Severmann, J. Huang, L. Feng, H. Chang, and Q. Zhang for laboratory and field assistance and helpful discussions. The NSF Earth Sciences program (grant EAR-0720362 to G.D.L. and T.W.L. and grant EAR-0719493 to A.L.S.), National Science Foundation of China Fund (grant 40532012 to X.C.), the Chinese Academy of Sciences Fund (grant KZCX3-SW-141 to X.C.), the NASA Astrobiology Institute, and the Agouron Institute provided funding.

Supporting Online Material

www.sciencemag.org/cgi/content/full/science.1182369/DC1
Materials and Methods
Figs. S1 to S7
Table S1
References

23 September 2009; accepted 27 January 2010
Published online 11 February 2010;
10.1126/science.1182369
Include this information when citing this paper.

Mantle Flow Drives the Subsidence of Oceanic Plates

Claudia Adam[1,2]* and Valérie Vidal[3]

The subsidence of the sea floor is generally considered a consequence of its passive cooling and densifying since its formation at the ridge and is therefore regarded as a function of lithospheric age only. However, the lithosphere is defined as the thermal boundary layer of mantle convection, which should thus determine its structure. We examined the evolution of the lithosphere structure and depth along trajectories representative of the underlying mantle flow. We show that along these flow lines, the sea-floor depth varies as the square root of the distance from the ridge (as given by the boundary-layer equation) along the entire plate, without any flattening. Contrary to previous models, no additional heat supply is required at the base of the lithosphere.

At mid-oceanic ridges, hot material rises and then cools while driven away to subduction zones, forming the tectonic plates. The structure of the lithosphere, as the upper thermal boundary layer, is determined by conductive cooling after its formation at the ridge. The lithosphere thickens away from the mid-oceanic ridge and, as rock density increases by cooling, slowly sinks into the underlying mantle. Therefore, the sea-floor depth is regarded as a function of its age only and is studied along trajectories following an age gradient (referred to as "age trajectories"). Several models have been proposed to describe the thermal subsidence of the sea floor with age (*1*–*4*), but no consensus has been reached on the origin of the flattening observed at old ages (*5*). These thermal subsidence models do not directly consider the role of convection in the underlying mantle, which deforms with a velocity on the order of a few centimeters per year. In particular, their description of passive lithosphere cooling ignores any change in plate motion (in other words, in mantle convection).

[1]Institute for Research on Earth Evolution, Japan Agency for Marine-Earth Science and Technology, 2-15 Natsushima, Yokosuka, 237-0061, Japan. [2]Centro de Geofísica, Universidade de Évora, Rua Romão Ramalho 59, 7002-554 Évora, Portugal. [3]Laboratoire de Physique, Université de Lyon, Ecole Normale Supérieure de Lyon–CNRS, 46 Allée d'Italie, 69364 Lyon cedex 07, France.

*To whom correspondence should be addressed. E-mail: adam@uevora.pt

The first model that proposed to explain the variations of sea-floor depth with age—the half-space model (*6*)—considered the lithosphere as the cold upper boundary layer of a cooling mantle, where the depth varies with the square root of the distance from the ridge. By assuming a constant plate velocity, the sea-floor depth varies with the square root of the age of the lithosphere. However, subsequent studies found that the observed sea-floor depth at old ages [>70 million years ago (Ma)] was substantially shallower than the model prediction (*1*, *2*). These studies suggested that the flattening observed at old ages could be accounted for by a model in which the lithosphere is considered as a rigid, cooling conductive plate with a constant basal temperature (plate model) (*2*, *3*, *7*). However, if this constant temperature at the base of the plate is a simple and convenient way to introduce the additional heat supply necessary to explain sea-floor flattening at old ages, there is no physical reason why this should be true for the entire plate. Different physical processes have been proposed to explain the origin of this additional heat supply: small-scale convection (*8*–*11*), upwelling mantle plumes (*12*, *13*), or internal heating, including radiogenic heating as well as the heating from secular cooling (*11*, *14*). Nonetheless, we still do not know which of these physical processes is truly responsible for the observed flattening at old ages.

Previous global models also do not account for possible variations of ridge temperature and depth, either spatial or temporal. Systematic studies of sea-floor subsidence along the East Pacific Rise, for instance, show that the ridge depth varies from 2000 to 3200 m, and the associated subsidence rate from 50 to 450 m/Ma$^{1/2}$ (*15*–*19*). These variations imply spatial mantle temperature variations of about ±100°C (*16*–*18*). Others suggested that the possible change through time of plate motion and plate-driving forces (*20*) [in particular, pulsations in sea-floor spreading rates (*21*), and a higher mean mantle temperature during the Mesozoic (*22*)] could be responsible for higher ridge height and subsidence rate during this period. Estimates of a mantle ~50°C warmer during the Mesozoic, for example, could explain much of the observed flattening relative to a boundary-layer model (*22*).

Regardless of their differences, all previous models are based on the hypothesis that the thermal structure of the oceanic lithosphere is determined entirely by its age—that is, the time elapsed since its creation at the mid-oceanic ridge. However, because mantle convection and plate motion evolve over time, the new thermal conditions imposed on the base of the oceanic lithosphere also change, thus modifying its structure. This lithospheric structure will evolve to adapt to the new thermal conditions imposed at its base, along the entire plate. After a drastic change in the convective system, it will either thicken (or, alternately, become thinner) if the temperature at its base, defined by the new convective system, is cooler (or hotter) than it was previously. After a time long enough (several tens of million years), the lithosphere will tend toward the structure of the thermal boundary layer for the new underlying mantle flow, independently of its initial state.

To test that the structure of the oceanic lithosphere is determined by the underlying mantle convection, we analyzed more than 770 depth profiles, leading to a complete coverage of the Pacific plate (*23*). Several kinematic models have been tested to compute the trajectories representative of the present-day mantle convection (flow lines) (*23*). The Pacific plate is an ideal candidate to test our hypothesis for a number of reasons. First, the Pacific plate velocity has remained constant over the last 47 to 50 million years (My) (*24*), providing sufficient time for the lithosphere to

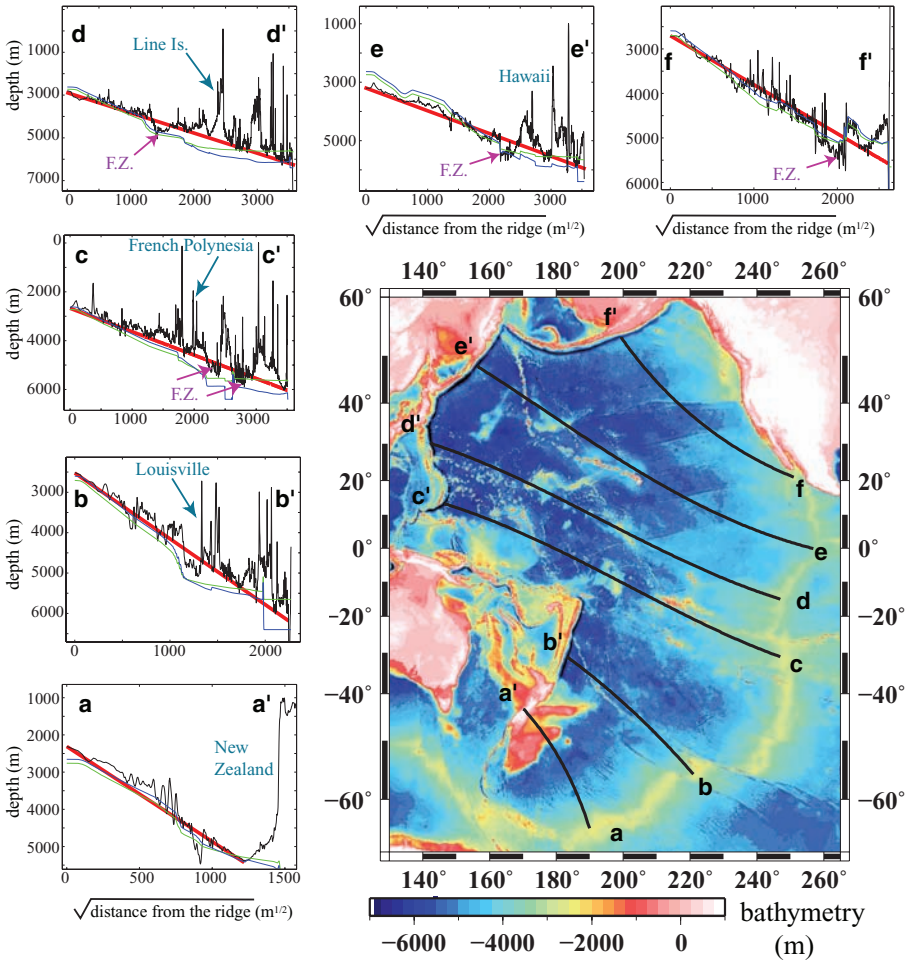

Fig. 1. (**Main panel**) Bathymetry of the Pacific plate (*27*) corrected for sediment loading and six examples of flow lines aa′, bb′, cc′, dd′, ee′, and ff′ (*23*). (**Side panels**) Profiles along the flow lines indicated in the main panel. Black, sea-floor depth as a function of the square root of the distance from the ridge; red, linear trend $z \propto x^{1/2}$; blue and green, models from (*2*) and (*3*), respectively. Arrows indicate the local geological features responsible for the departure from the linear trend (F.Z. indicates a fracture zone).

adapt to the new thermal conditions. Second, the drastic change in its motion, which is the consequence of a large-scale rearrangement of the mantle convection 47 to 50 million years ago (*24*), has necessarily induced an important change in the thermal conditions applied to the older lithosphere. Therefore, flow lines, which are representative of the underlying mantle convection, strongly differ from age trajectories. Third, the large size of the Pacific plate provides us with the longest observable oceanic lithosphere temporal and spatial evolution on the planet. Finally, because of the strong driving force provided by its slab morphology and trench length, the Pacific has the fastest plate velocity (*25*). If mantle convection is the driving mechanism of sea-floor subsidence, its effects will be most visible over this plate.

Along the flow lines (Fig. 1), we observe a linear relation between the sea-floor depth (z) and the square root of the distance from the ridge ($x^{1/2}$), written as

$$z = z_R + ax^{1/2} \quad (1)$$

where z_R is the ridge depth, and a is the subsidence rate. This relation holds true all along the plate, from the ridge where it forms to the subduction zone where it sinks into the mantle. Departures from the linear trend are localized (Fig. 1) and can be explained by local geophysical processes. The highs are associated with volcanoes (isolated seamounts, hot-spot chains) and swells due to buoyant mantle upwelling (including the South Pacific Superswell). The lows are correlated to the flexure of the lithosphere due to volcano loading or to fracture zones. In all cases, the wavelength of these anomalies is much shorter than the general trend (Fig. 1).

Along the flow lines, no flattening is observed at old ages, far away from the ridge. Despite de-

Fig. 2. (**Right**) Sea-floor age (*28*), flow lines (black lines), and age trajectories (white lines) (*23*). (**Left**) Depth profiles along the age trajectories. Black, sea-floor depth as a function of the square root of the sea-floor age; red, our model; blue and green, models from (*2*) and (*3*), respectively. Our model (red line) fits the general trend of the bathymetry along the entire plate. Contrary to previous models, there is no need to invoke any flattening at old ages.

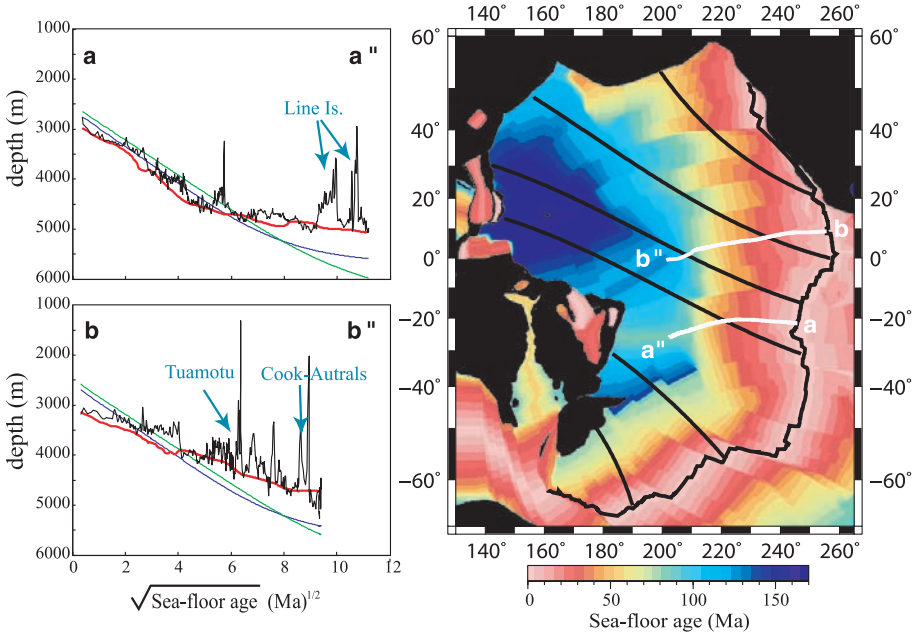

partures from the model due to local processes, the thermal subsidence along the present-day convective motion direction follows the expected trend. Over the Pacific plate, the flow lines strongly differ from the age trajectories (Fig. 2), which is the key point to discriminate our analysis from previous models. Along the age trajectories, the depth profiles represented in Fig. 2 [based on a continuous grid (*23*)] show that there is an apparent flattening. But this flattening is only due to the misleading direction along which the subsidence is investigated. Contrary to previous models (*2*, *3*), our model fits the general trend of the bathymetry along the entire plate. The subsidence rates found in this study vary from 0.5 to 3.5 $m/m^{1/2}$. Rescaling by the constant Pacific plate velocity (9 cm $year^{-1}$) gives values ranging from 200 to 900 $m/Ma^{1/2}$, comparable to the values found in previous studies (*15*–*19*).

The general trend of the sea-floor depth along flow lines, representative of the underlying mantle convection, validates our hypothesis that the lithosphere should be viewed as the upper thermal boundary layer of mantle convection, its true definition (*26*). Because of the steady-state conditions imposed during the last 47 to 50 My (*24*), the Pacific lithosphere had time to readjust, by conduction, to the thermal conditions imposed at its base by the underlying convective mantle. The structure of the lithosphere (and, hence, its thermal subsidence) is therefore driven by the underlying mantle flow. This simple alternative perspective contrasts to the many more complicated explanations that have previously been proposed. In particular, we find that there is no sea-floor flattening at old ages and, therefore, no need to invoke any additional heat supply at the base of the old lithosphere.

References and Notes

1. J. G. Sclater, L. A. Lawver, B. Parsons, *J. Geophys. Res.* **80**, 1031 (1975).
2. B. Parsons, J. G. Sclater, *J. Geophys. Res.* **82**, 803 (1977).
3. C. A. Stein, S. Stein, *Nature* **359**, 123 (1992).
4. M.-P. Doin, L. Fleitout, *Earth Planet. Sci. Lett.* **142**, 121 (1996).
5. M.-P. Doin, L. Fleitout, *Geophys. J. Int.* **143**, 582 (2000).
6. R. L. Parker, D. W. Oldenburg, *Nature* **242**, 137 (1973).
7. A. G. Crosby, D. McKenzie, J. G. Sclater, *Geophys. J. Int.* **166**, 553 (2006).
8. B. Parsons, D. McKenzie, *J. Geophys. Res.* **83**, 4485 (1978).
9. D. A. Yuen, L. Fleitout, *Nature* **313**, 125 (1985).
10. M. A. Eberle, D. W. Forsyth, *Geophys. Res. Lett.* **22**, 473 (1995).
11. J. Huang, S. Zhong, *J. Geophys. Res.* **110**, B05404 (2005).
12. W. Schroeder, *J. Geophys. Res.* **89**, 9873 (1984).
13. G. F. Davies, *J. Geophys. Res.* **93**, 10467 (1988).
14. G. F. Davies, M. A. Richards, *J. Geol.* **100**, 151 (1992).
15. J. C. Marty, A. Cazenave, *Earth Planet. Sci. Lett.* **94**, 301 (1989).
16. B. Lago, A. Cazenave, J. C. Marty, *Phys. Earth Planet. Inter.* **61**, 253 (1990).
17. K. A. Kane, D. E. Hayes, *J. Geophys. Res.* **99**, 21759 (1994).
18. K. Perrot, J. Francheteau, M. Maia, C. Tisseau, *Earth Planet. Sci. Lett.* **160**, 593 (1998).
19. J. R. Cochran, W. R. Buck, *J. Geophys. Res.* **106**, 19233 (2001).
20. C. P. Conrad, C. Lithgow-Bertelloni, *J. Geophys. Res.* **109**, B10407 (2004).
21. S. R. Gaffin, B. C. O'Neill, *Geophys. Res. Lett.* **21**, 1947 (1994).
22. E. Humler, C. Langmuir, V. Daux, *Earth Planet. Sci. Lett.* **173**, 7 (1999).
23. Supporting material is available on *Science* Online.
24. W. D. Sharp, D. A. Clague, *Science* **313**, 1281 (2006).
25. A. E. Gripp, R. G. Gordon, *Geophys. Res. Int.* **150**, 321 (2002).
26. T. Turcotte, G. Schubert, *Geodynamics* (Cambridge Univ. Press, Cambridge, ed. 2, 2002).
27. W. H. F. Smith, D. T. Sandwell, *Science* **277**, 1956 (1997).
28. R. D. Müller, W. R. Roest, J.-Y. Royer, L. M. Gahagan, J. G. Sclater, *J. Geophys. Res.* **102**, 3211 (1997).

29. We thank A. Bonneville, F. Lucazeau, and Y. Fukao for fruitful discussions.

Supporting Online Material

www.sciencemag.org/cgi/content/full/328/5974/83/DC1
SOM Text
Figs. S1 and S2
References

14 December 2009; accepted 18 February 2010
10.1126/science.1185906

Orchestration of Floral Initiation by APETALA1

Kerstin Kaufmann,[1,2]* Frank Wellmer,[3]* Jose M. Muiño,[4] Thilia Ferrier,[5] Samuel E. Wuest,[3] Vijaya Kumar,[6] Antonio Serrano-Mislata,[7] Francisco Madueño,[7] Pawel Krajewski,[8] Elliot M. Meyerowitz,[6] Gerco C. Angenent,[1,9] José Luis Riechmann[5,6,10]†

The MADS-domain transcription factor APETALA1 (AP1) is a key regulator of *Arabidopsis* flower development. To understand the molecular mechanisms underlying AP1 function, we identified its target genes during floral initiation using a combination of gene expression profiling and genome-wide binding studies. Many of its targets encode transcriptional regulators, including known floral repressors. The latter genes are down-regulated by AP1, suggesting that it initiates floral development by abrogating the inhibitory effects of these genes. Although AP1 acts predominantly as a transcriptional repressor during the earliest stages of flower development, at more advanced stages it also activates regulatory genes required for floral organ formation, indicating a dynamic mode of action. Our results further imply that AP1 orchestrates floral initiation by integrating growth, patterning, and hormonal pathways.

Phase transitions in plants require the reprogramming of meristematic identities (*1*). Although several key regulators involved in this process have been identified, their molecular modes of action remain largely elusive. The floral meristem identity gene *APETALA1* (*AP1*) and its paralog *CAULIFLOWER* (*CAL*) control the onset of *Arabidopsis* flower development in a partially redundant manner (*2*). When both genes are mutated, plants do not transition to flowering but instead exhibit massive overproliferation of inflorescence meristems, leading to a cauliflower-like appearance. *AP1* expression is first observed throughout emerging floral primordia and is later confined to the outer whorls of floral buds, where AP1 is involved in the specification of sepals and petals (*3*). Several transcription factors have been identified that bind directly to the *AP1* promoter and control the onset of its expression. These include the floral meristem identity factor LEAFY (LFY) (*4*), the basic leucine zipper (bZIP) protein FD in concert with FLOWERING LOCUS T (FT) (*5*, *6*), as well as members of the SQUAMOSA PROMOTER BINDING PROTEIN-LIKE (SPL) family (*7*, *8*).

Previous studies have provided first insights into AP1 function during early flower development. AP1 directly represses the flowering time genes *SHORT VEGETATIVE PHASE* (*SVP*), *AGAMOUS-LIKE24* (*AGL24*), and *SUPPRESSOR OF OVEREXPRESSION OF CO1* (*SOC1*) in emerging floral primordia (*9*). Furthermore, it represses, directly or indirectly, the shoot identity gene *TERMINAL FLOWER1* (*TFL1*) (*10*), promotes the transcription of *LFY* as part of a positive feedback loop (*10*), and controls the expression of floral homeotic genes (*11*, *12*).

To obtain a detailed understanding of AP1 function during floral initiation, we identified genes that are controlled by it on a genome-wide scale. We used a previously described line expressing a fusion between AP1 and the hormone-binding domain of a glucocorticoid receptor (AP1-GR) in an *ap1 cal* double-mutant

[1]Business Unit Bioscience, Plant Research International, Wageningen 6700 AA, Netherlands. [2]Laboratory of Molecular Biology, Wageningen University, Wageningen 6700 AP, Netherlands. [3]Smurfit Institute of Genetics, Trinity College, Dublin 2, Ireland. [4]Applied Bioinformatics, Plant Research International, Wageningen 6700 AA, Netherlands. [5]Center for Research in Agricultural Genomics (CRAG), Barcelona 08034, Spain. [6]California Institute of Technology, Division of Biology, Pasadena, CA 91125, USA. [7]Instituto de Biología Molecular y Celular de Plantas, Consejo Superior de Investigaciones Científicas–Universidad Politécnica de Valencia, Valencia 46022, Spain. [8]Institute of Plant Genetics, Polish Academy of Sciences, Poznan 60-479, Poland. [9]Centre for BioSystems Genomics (CBSG), Wageningen 6700 AB, Netherlands. [10]Institució Catalana de Recerca i Estudis Avançats, Barcelona 08010, Spain.

*These authors contributed equally to this work.
†To whom correspondence should be addressed. E-mail: jriechma@caltech.edu